

Phase evolution and microstructural development in sol-gel derived MSnO_3 ($\text{M} = \text{Ca}, \text{Sr}$ and Ba)

A.-M. AZAD*, M. HASHIM, S. BAPTIST†

Department of Physics, University Putra Malaysia, 43400 UPM Serdang, Selangor, Malaysia
E-mail: abmajeed.azad@hotmail.com

A. BADRI

Department of Metallurgical Engineering, McGill University, Quebec, Canada

A. UL. HAQ

Metallurgy Division, Dr. A.Q. Khan Research Laboratories, Kahuta, P.O. Box 502 Rawalpindi, Pakistan

Alkaline-earth stannates having the general chemical formula MSnO_3 ($\text{M} = \text{Ca}, \text{Sr}$ and Ba) have been projected as potential electronic ceramics. In view of the information gaps in the reported research, a vigorous and systematic investigation on these exotic materials has been carried out. In this communication, the synthesis of CaSnO_3 , SrSnO_3 and BaSnO_3 via sol-gel technique is reported. Infrared spectroscopy and X-ray analyses of various gel samples with different thermal history helped in identifying the reaction pathways and the stage where amorphous gel to crystalline phase transition occurred. Grains of submicron size with narrow size distribution and spherical morphology, were the most noticeable characteristics of sintered calcium metastannate derived by sol-gel method. In the case of barium analogue, a fascinating 'sugar cube' structure (akin to that observed in solid-state reaction and the self-heat-sustained reaction derived samples) having improved density characteristics evolved at low sintering temperatures. This gradually transformed into a more familiar spherical granular motif with improved density characteristics as the sintering profiles were varied from 1200 °C/24 h to 1500 °C/2 h. This seems to be an inherent feature of this system, irrespective of the method of synthesis. © 2000 Kluwer Academic Publishers

1. Introduction

The alkaline earth stannates (MSnO_3) belong to a series of dielectric material components used for thermally stable capacitors in electronic industry [1]. There is a great scope of exploiting heterojunctions of these stannates with other suitable oxides as capacitive sensors for carbon dioxide detection and metering and other gas sensing devices [2, 3]. Recently, Ostrick *et al.* [4] have reported results of Hall measurements on BaSnO_3 at high temperatures to elucidate the nature of defects prevailing in the material. The energy band gap in these stannates is about 3.0–3.5 eV, which is well within the range generally desired for gas sensor materials [5]. Suggestions have also been made that, by combining BaTiO_3 with BaSnO_3 (BTS), multifunctional ceramic sensors can be developed which can detect temperature, relative humidity, and gases such as acetylene and ethylene at ambient temperatures and pressures [6].

Despite such technological importance, any information on processing and evolution of microstructure in these materials and their impact on the electrical characteristics are lacking in the literature. Parkash *et al.* [7],

Mandal *et al.* [8] and Upadhyay *et al.* [9] have reported electrical measurements on CaSnO_3 , SrSnO_3 and BaSnO_3 samples, at three 'spot' frequencies, viz., 1, 10 and 100 kHz only. Thus, there is a noticeable lack of correlation among synthesis, processing and microstructural aspects of MSnO_3 compounds with their electrical characteristics. Hence, a vigorous systematic study to fill in the information gap on these materials of technological importance was initiated and the detailed investigations have recently been reported elsewhere [10–15]. In this communication, the synthesis of MSnO_3 ($\text{M} = \text{Ca}, \text{Sr}$ and Ba) compounds using the sol-gel technique and their characterization by IR and XRD methods is reported. The evolution of microstructure in calcium and barium stannates under various sintering conditions is also presented.

2. Experimental

2.1. Compound synthesis

2.1.1. CaSnO_3

2.1.1.1. *Ca-Sn acetate gel.* Calcium acetate (99%+, Pi-Kem, Surrey, UK) and tin (IV) acetate (97%+,

* Author to whom all correspondence should be addressed. Current address: Dept. of Materials Science & Engg., University of Florida, 100 Rhines Hall, Gainesville, FL 32611-6400 USA. Email: aazad@mse.ufl.edu

† Present Address: Nilai College, No. 1, Persiaran Kolej BBN, 71800 Bandar Baru Nilai, Negeri Sembilan, Malaysia.

Pi-Kem, Surrey, UK) were dissolved separately in glacial acetic acid (BDH, India) under constant stirring. The two clear solutions were subsequently mixed together and stirred overnight to obtain a homogeneous solution of the two acetates. Distilled water in the concentration ratio, $[H_2O]/[M]$, ranging between 4 to 4.5, was slowly added to the solution to assist the hydrolysis of the mixed acetate. The mixture was kept under constant stirring at room temperature for 6 h after water addition and the temperature of the sol was slowly raised and maintained at 70 °C. A colorless transparent gel was seen formed slowly from the viscous liquid. During the last stages of gelation (indicated by enhanced viscosity) stirring was terminated and natural evaporation was allowed to form the gel. The gel was subsequently dried in an air oven at 110 °C overnight to drive off remnant acetic acid and water.

2.1.1.2. Ca-Sn ethoxide gel. Calcium ethoxide ($Ca(OC_2H_5)_2$, 99.5%, lot # 95182, Pi-Kem, Surrey, UK) and tin (II) ethoxide (batch # 2225, Pi-Kem) were dissolved separately in adequate amount of extra pure absolute ethanol (C_2H_5OH , batch # 228171, Scharlau, Barcelona, Spain) with moderate stirring at room temperature for 3 h. The other experimental details are similar to those described above in the case of acetate gel.

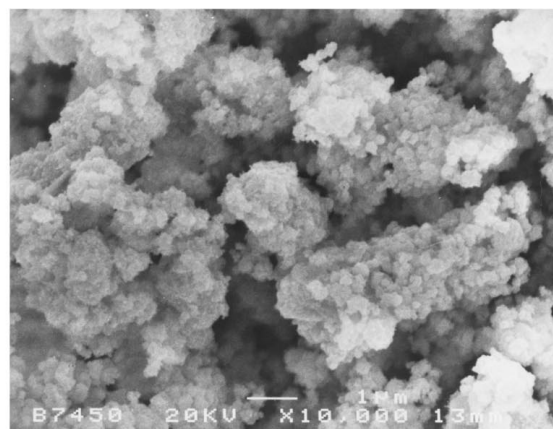
2.1.2. $SrSnO_3$

2.1.2.1. Sr-Sn acetate gel. One of the starting materials, viz., strontium acetate, $Sr(OOCCH_3)_2$, was synthesized from the readily available $Sr(NO_3)_2$. Anhydrous $Sr(NO_3)_2$ (99%, BDH, Poole, UK) was dissolved in minimum amount of distilled water. Slight excess of glacial acetic acid was added to the aqueous solution and stirred moderately for 3 h. Tin (IV) acetate (Pi-Kem, Surrey, UK) was also similarly dissolved in glacial acetic acid separately. The two solutions were mixed and stirred for another 3 h. Distilled water was added in small aliquots to the mixed acetate solution in excess of the stoichiometric requirement (determined by several trial experiments) for the hydrolysis of the mixed acetate. The mixture was kept under constant stirring at room temperature for 6 h after water addition and the temperature of the sol was slowly raised and maintained at 60–70 °C with constant stirring. The onset of the formation of a transparent gel was observed after several hours, which gradually became increasingly viscous. During the last stages of gelation (indicated by enhanced viscosity) stirring was terminated and natural evaporation was allowed to form the gel. The gel was dried in an air oven at 110 °C overnight to drive off remnant acetic acid and water.

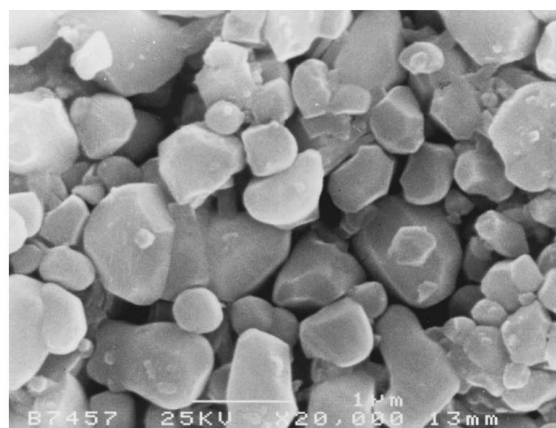
2.1.3. $BaSnO_3$

2.1.3.1. Ba-Sn ethoxide gel. Barium ethoxide, ($Ba(OC_2H_5)_2$, 99.5%, lot # 96101, Pi-Kem, Surrey, UK) and tin (II) ethoxide (batch # 2225, Pi-Kem) were dissolved separately in adequate amount of extra pure absolute ethanol (C_2H_5OH , batch # 228171, Scharlau, Barcelona, Spain) with moderate stirring at room

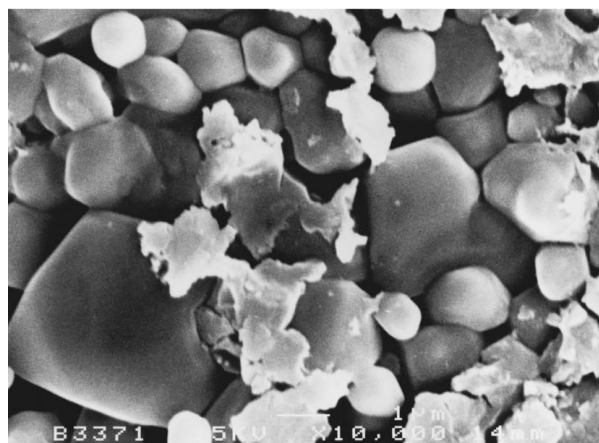
temperature for 3 h. The two solutions were mixed and stirred overnight. Distilled water was added in small aliquots to the mixed ethoxide solution in excess of the stoichiometric requirement (determined by several trial experiments) for the hydrolysis of the mixed ethoxide. The mixture was kept under constant stirring at room temperature for 6 h after water addition and the temperature of the sol was slowly raised and maintained at 70 °C with constant stirring. The resulting transparent gel was dried in an air oven at 110 °C overnight to drive off remnant ethanol and water.



(a)



(b)



(c)

Figure 1 Comparison of morphology in calcium stannate from solid-state (a) and self-heat-sustained (b) reaction route with that in sol-gel derived precursor (c).

2.2. Characterization

Small portions of the dried gel in each stannate were calcined at various temperatures ranging between 200 to 900 °C for 2 or 4 h. Infrared spectroscopic examination of the dried as well as the calcined gel was performed, using a Perkin-Elmer instrument in the range 4000–400 cm^{-1} , in order to determine the lowest temperature at which amorphous to crystalline phase transformation occurred. Each of these samples was also subjected to X-ray analyses to confirm the gel to crystalline transformation and to ascertain the lowest temperature at which this occurred. X-ray diffraction patterns were extracted on powder samples (dried gels as well as those calcined at different temperatures for small duration), in the range 10–90° (2θ), using $\text{Cu K}\alpha$ radiation and Ni filter, at a scan rate of 1° (2θ) per min.

The calcined gel powders was subjected to sintering (in order to follow the evolution of microstructure) at 3 different temperatures in the range 1200 to 1500 °C for duration ranging from 2 h to 48 h in ambient air. Prior

to sintering, the calcined powder was blended with 1 wt. % polyvinyl alcohol (PVA) as binder, dried under UV lamp and compacted into green pellets of 1–2 mm thickness and 6 mm diameter, by pressing in stainless steel dies at pressures not exceeding 50 MPa.

Microstructural features of the dry gel powders as well as the sintered discs were determined by using a JEOL-6400SM (Japan) scanning electron microscope (SEM). In the case of powder, the specimen was evenly sprinkled on the glued surface of an aluminum stub. In the case of sintered samples, the pellets were mounted flat on the aluminum stub without polishing or etching, so as to expose the surface to the incident electron beam in the microscope. A uniform thin film of gold was evaporated on the surface by Polaron Coating Machine (UK), to avoid electrostatic charging during microscopic viewing. From the rate and time of evaporation, the thickness of the gold coating was estimated to be about 10–30 Å. Owing to the strong susceptibility of these compounds toward moisture,

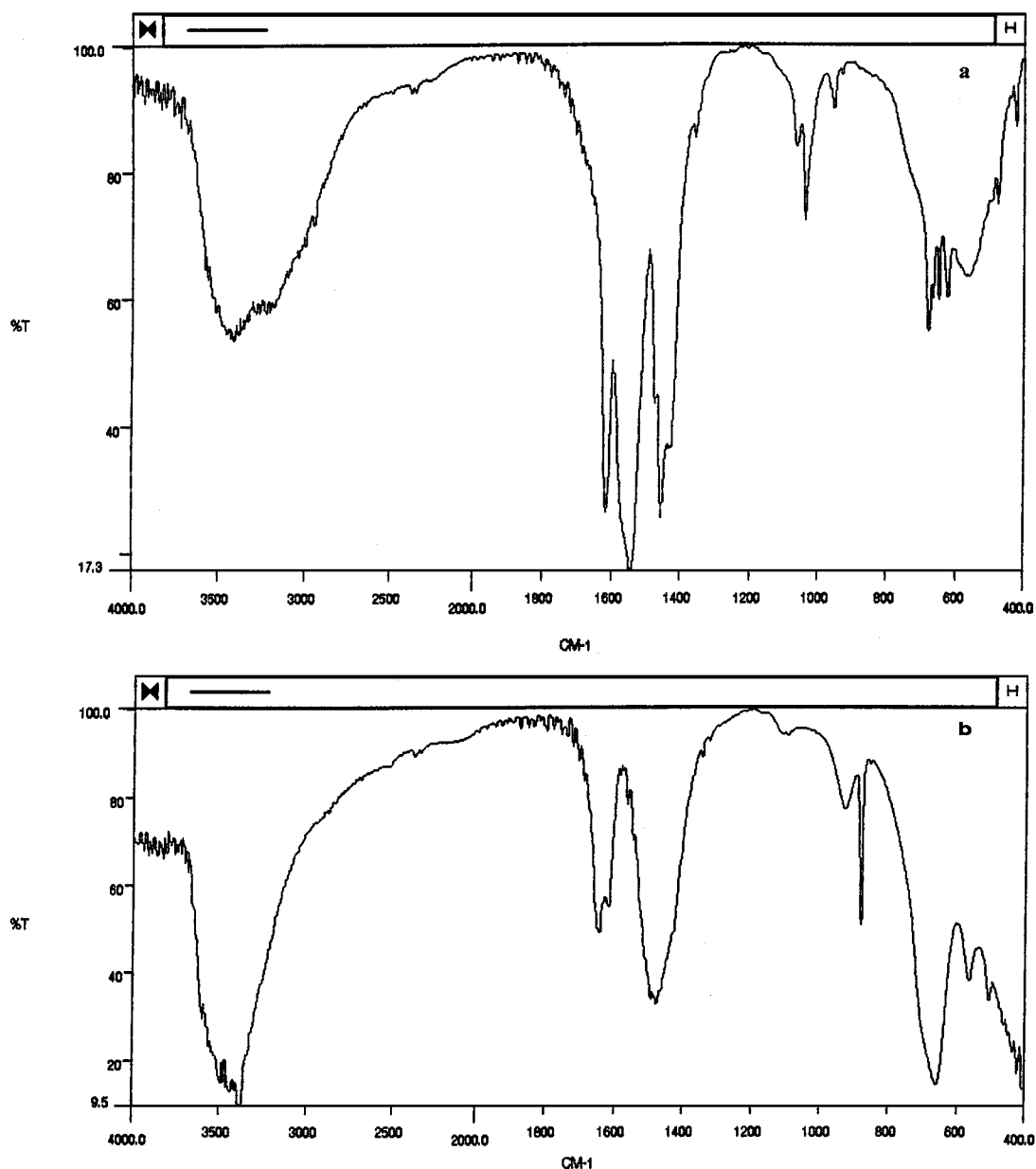


Figure 2 Variation in infrared spectroscopic signatures in Ca-Sn acetate gel as a function of calcination temperature: (a) dried gel and (b) 800 °C/4 h.

the calcined powder as well as the sintered discs were always stored in the humidity-free bottles containing anhydrous CaCl_2 , unless required for structural or microscopic measurements.

3. Results and discussion

3.1. CaSnO_3

3.1.1. Characterization of dried and calcined gel

The morphology of the particles in the dried gel obtained from hydrolysis of mixed acetates is compared

with that of the CaSnO_3 raw powders derived from the solid-state and self-heat-sustained (SHS) reaction techniques in Fig. 1. While the green powder from solid state reaction is in the form of agglomerates of crystallites of uniform and very small (sub-micron) size (Fig. 1a), that obtained via SHS technique has very distinct features in that SHS yielded individual grains of definite crystalline orientation (Fig. 1b); the grain size distribution was rather narrow (average size $\sim 0.5 \mu\text{m}$). In contrast to this, the morphology of the particles in the dried gel shows individual, nearly perfect spherical grains with average grain being less than $1 \mu\text{m}$ in size (Fig. 1c).

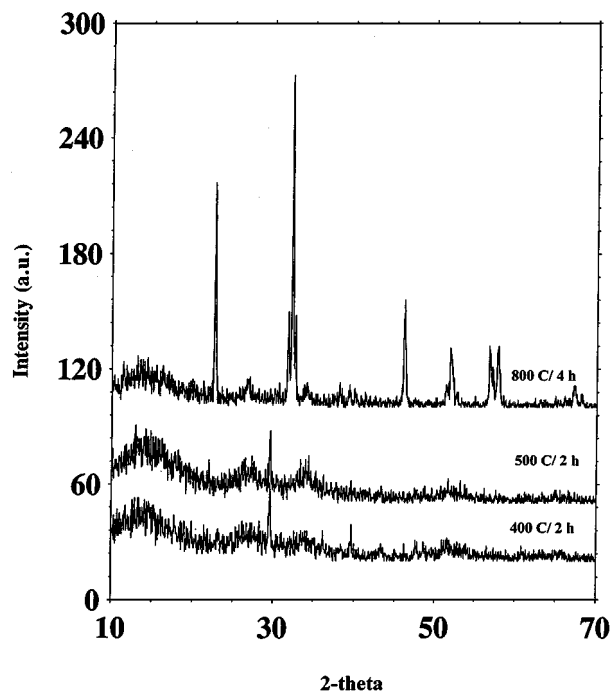


Figure 3 Progress of the evolution of crystalline phase in Ca-Sn acetate gel with calcination temperature.

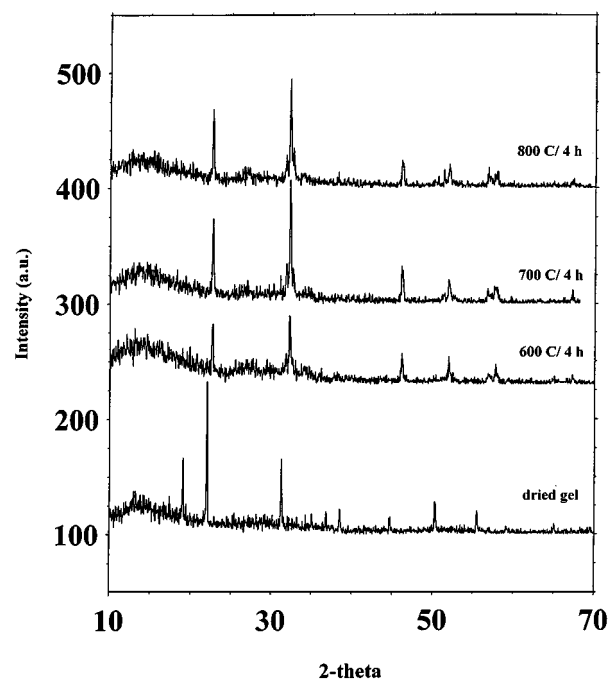
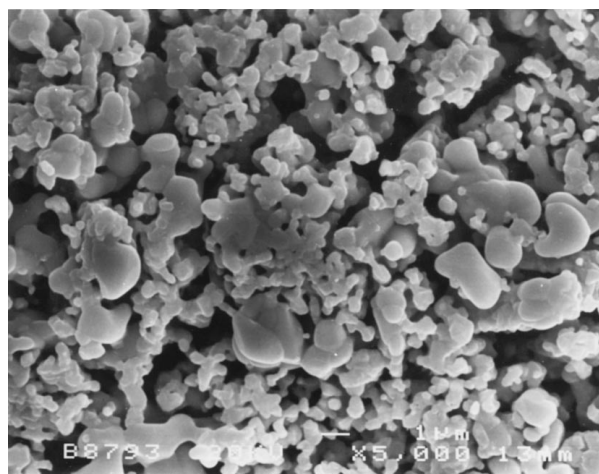
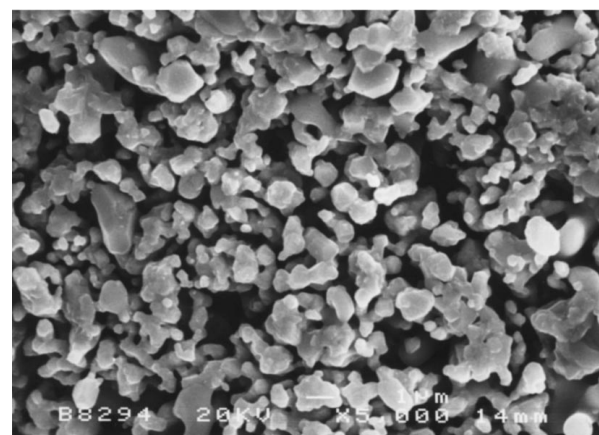


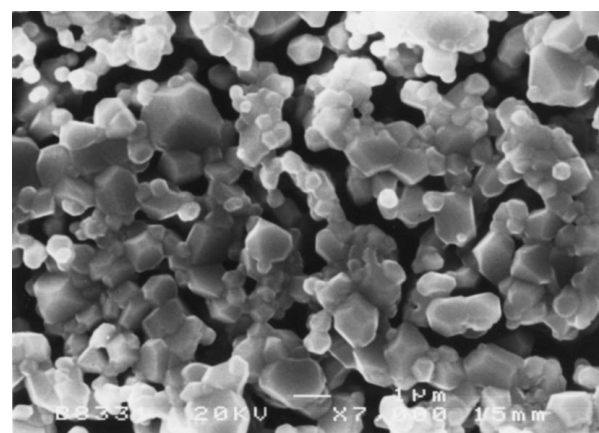
Figure 4 Progress of the evolution of crystalline phase in Ca-Sn ethoxide gel with calcination temperature.



(a)



(b)



(c)

Figure 5 Microstructure of acetate gel-derived CaSnO_3 soaked at (a) 1200°C for 12 h, (b) 1200°C for 48 h and (c) 1300°C for 12 h.

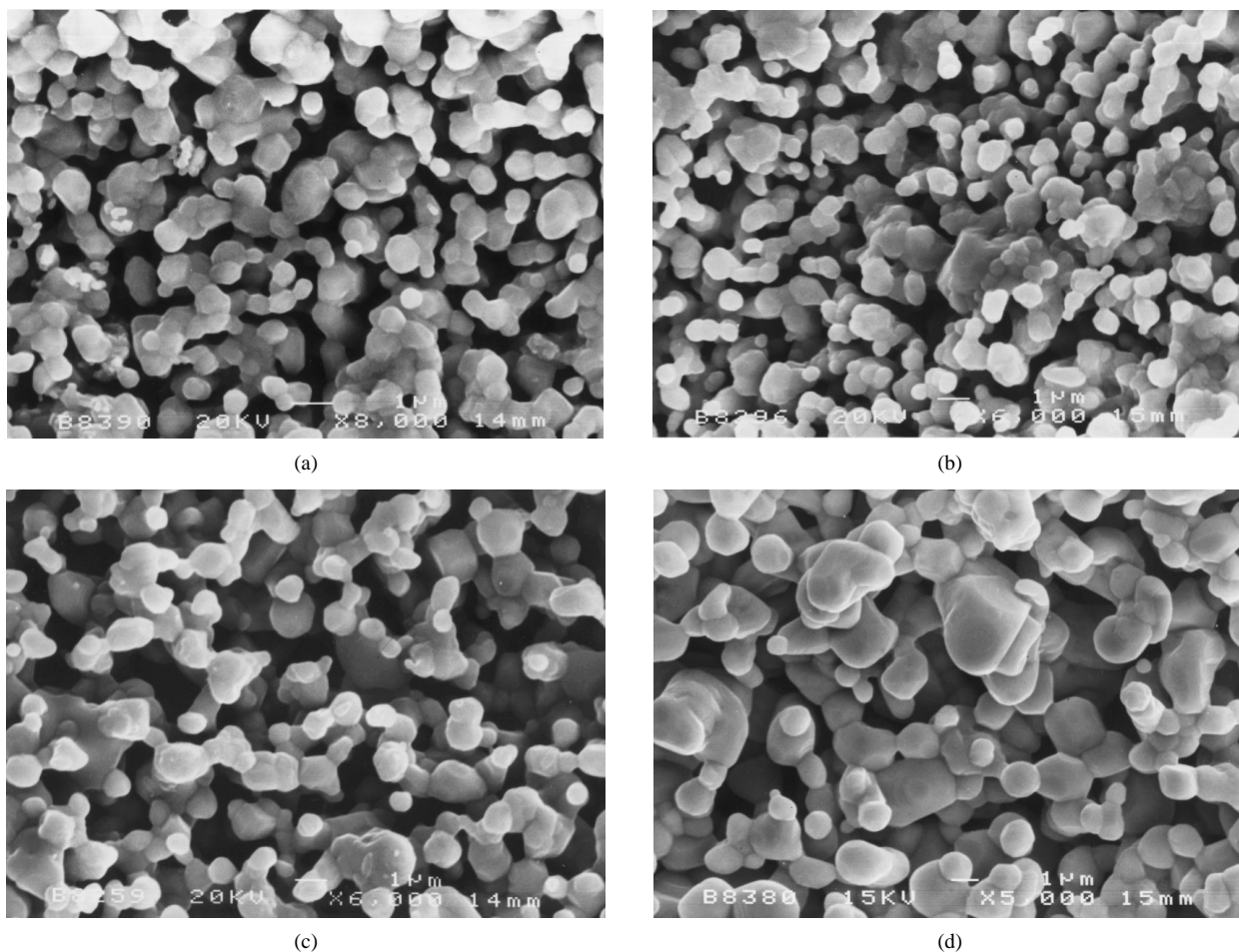


Figure 6 Microstructure of ethoxide-gel derived CaSnO_3 soaked at (a) $1200\text{ }^\circ\text{C}$ for 24 h, (b) $1200\text{ }^\circ\text{C}$ for 48 h, (c) $1300\text{ }^\circ\text{C}$ for 6 h and (d) $1300\text{ }^\circ\text{C}$ for 12 h.

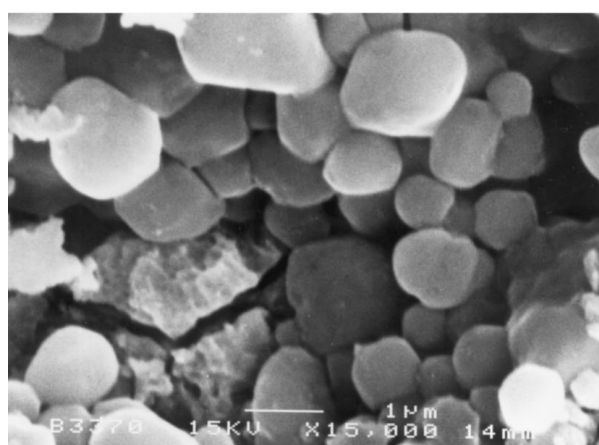


Figure 7 Morphology of sol-gel derived SrSnO_3 from acetate precursors.

In order to ascertain the onset of evolution of crystalline phase from the amorphous gel, the latter calcined at different temperatures for small duration, was subjected to IR and XRD analyses. The IR spectra of the dry as well as the calcined gel, shown in Fig. 2, clearly shows the progress of gel-to-crystalline transformation, in terms of the diminishing peaks due to carboxylate ions (from acetate complex) which were bidentately linked to the metal ions and those due to hydroxyl ions in the hydrolyzed precursor. The IR signature of the hy-

drolyzed calcium tin acetate gel calcined at $800\text{ }^\circ\text{C}$ for 4 h, tallies well with that reported in the literature [16] for calcium metastannate, CaSnO_3 . The corresponding XRD pattern extracted on the dry and the calcined gel does not show the beginning of crystallinity up to $500\text{ }^\circ\text{C}$ (Fig. 3). The XRD signature corresponding to the standard JCPDS card on CaSnO_3 , is obtained on the gel calcined at $800\text{ }^\circ\text{C}$ for 4 h, thereby corroborating the IR results. Thus, CaSnO_3 could be synthesized in phase pure form by calcining the hydrolyzed acetate gel at temperature as low as $800\text{ }^\circ\text{C}$ for 4 h. This can be compared with the temperature of $1000\text{ }^\circ\text{C}/24\text{ h}$ and $1200\text{ }^\circ\text{C}/24\text{ h}$ needed for compound formation in the case of solid-state and SHS route, respectively [12].

The ethoxide-derived calcium stannate gels were also calcined between 200 and $800\text{ }^\circ\text{C}$ for 4 h. The XRD patterns of these as well as the dried gel is shown in Fig. 4. The diffraction signatures of the gels calcined up to $500\text{ }^\circ\text{C}/4\text{ h}$, remained akin to that of the dried gel (and hence are omitted here), indicating that gel to crystalline transformation has not set in at least up to a temperature of $500\text{ }^\circ\text{C}$. It can be seen that in the case of ethoxide gel, the formation of compound CaSnO_3 began at about $600\text{ }^\circ\text{C}$; calcination at temperatures higher than this, led only to the sharpening and increase in intensity of the peaks, without any change in the peak positions. It therefore, follows that the ethoxide precursor method is superior to its acetate counterpart in the sense that

the inception of compound formation began and was completed at much lower temperature. A comparison of the XRD patterns of the CaSnO_3 obtained on acetate and ethoxide derived gels calcined at 800°C for 4 h, indicates a more well-defined structure in the case of acetate precursors as the starting materials. Moreover, in terms of the economy of the process, metal acetate precursors are much less expensive than the corresponding ethoxides; therefore, even though the gel-to-crystalline transformation and the compound formation began at 600°C in the case of ethoxide gel, the better quality of the end product in the case of acetate precursor qualifies it to be the favorite starting material for sol-gel synthesis of CaSnO_3 . However, the microstructural features in the sintered bodies derived from the two different starting organometallic sources are quite different. In terms of intergranular connectivity and progressive densification, the gel obtained from the ethoxide route seems to be more benign. These aspects are discussed in the following subsection.

3.1.2. Microstructure in sintered bodies

As shown in Fig. 1c, the dried gel morphology consists of distinctly individual grains, predominantly submicron in size with near perfect sphericity. However, such favorable morphology did not lead to any systematic microstructure in the calcium stannate derived from acetate gels, which were sintered at 1200°C for 12–48 h and at 1300°C for 6–12 h. Fig. 5 shows some typical microstructures to illustrate this point. At 1200°C the compacts consist mainly of agglomerates of submicron-sized and a few overgrown grains (Fig. 5a and b). The structure also has a high degree of porosity. Sintering at 1300°C for 12 h (Fig. 5c) evidently leads to grain growth due to enhanced diffusion and results in highly angular crystallites, many of them $>1\ \mu\text{m}$ in size. However, the majority of the grains still have size $<1\ \mu\text{m}$ while the structure consisted of agglomerates and showed significant porosity.

Fig. 6 shows the microstructural evolution in ethoxide gel powder compacts sintered at $1200\text{--}1300^\circ\text{C}$ for

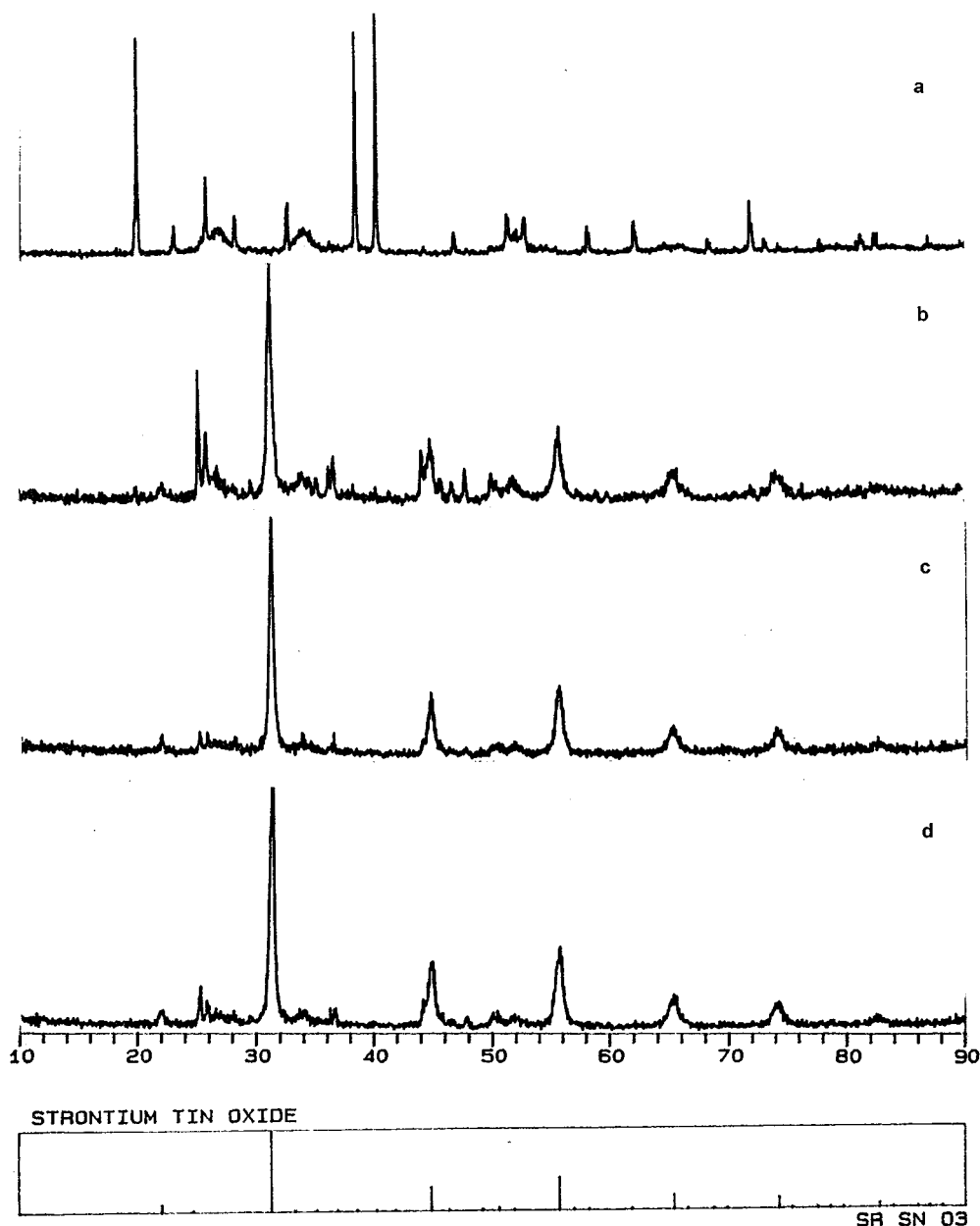


Figure 8 Powder X-ray patterns of SrSnO_3 samples synthesized via acetate precursor; a–d refer to the gels calcined for 2 h at 400, 500, 600 and 700°C respectively.

various soak-time. In contrast to the development in the acetate-derived gels, the microstructure of the sintered ethoxide powder consists of well-connected predominantly spherical grains. There is not significant grain growth up to 6 h soak-time at 1300 °C. The grain-to-grain connectivity improved significantly in samples sintered at 1300 °C for 12 h accompanied by some grain growth and corresponding decrease in open porosity. Thus, it appears that for better intergranular connectivity and densification, powders derived via ethoxide precursors are more benign.

3.2. SrSnO₃ gel

3.2.1. Characterization of dried and calcined gel

The morphology of the dried SrSnO₃ gel is shown in Fig. 7. The nearly perfect spherical shape of the grains of submicron dimensions can be clearly seen. The IR spectrum of the dried gel showed a rather strong absorption band at 815 cm⁻¹ and a weaker one at 1385 cm⁻¹, typical of nitrate ions, corresponding to ν_1 and ν_2 mode, respectively [16]. The presence of carboxylate ions (from acetate complex) which were bidentately linked to the metal ions, was evidenced by peaks at 1439, 1635–1637, 1791 and 2427 cm⁻¹. With increase in calcination temperature, the peaks at stretching frequencies of ν_2 modes of carbonate ion in the range 880–1440 cm⁻¹, progressively decrease (e.g., from ~22–91% in the dried gel to ~1–16% in the sample calcined at 500 °C). The IR spectrum of the gel calcined at 600 °C for 2 h had distinct absorption peaks at 660, 860, 1450 and, 1770 cm⁻¹ matching with those reported for SrSnO₃ [16]. This implied that the onset of conversion of amorphous gel to crystalline SrSnO₃ probably began at 500 °C and was complete by 600 °C.

Fig. 8 shows the evolution of X-ray diffraction pattern in samples heated at 400, 500, 600 and 700 °C for 2 h each. The XRD signatures of gel heated up to 300 °C were typical of amorphous samples. This indicated that gel (amorphous) to crystalline transformation did not begin up to 300 °C. The first indication of crystal formation (though not the compound formation) is shown by the XRD of the gel heated at 400 °C. Appearance of the diffraction peaks corresponding to the targeted compound begins at 500 °C and the formation of phase pure SrSnO₃ is confirmed by the XRD pattern taken on the gel heated at 600 °C; the presence of very sharp peaks suggests the formation of very small crystallites as expected in a sol-gel based synthesis. Heating the gel to 700 °C does not alter the XRD except that more sharper (in terms of the intensity) peaks identical to those on 600 °C/2 h samples are seen. This corroborates and confirms that SrSnO₃ could be synthesized in pure form via sol-gel technique at temperatures as low as 600 °C in relatively short time. This by far is the most attractive synthesis route, yielding high purity powder with small crystallite size. The microstructural investigation on the sintered SrSnO₃ samples is underway and the results will be reported in a separate communication.

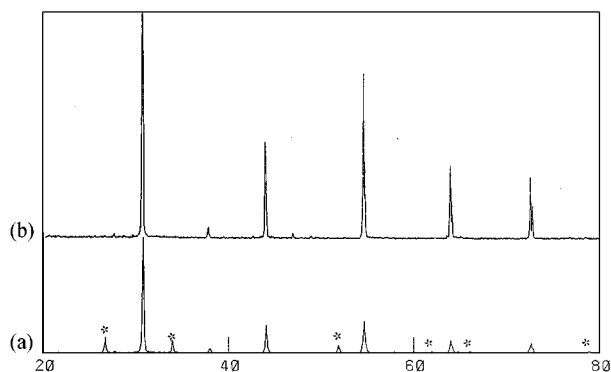
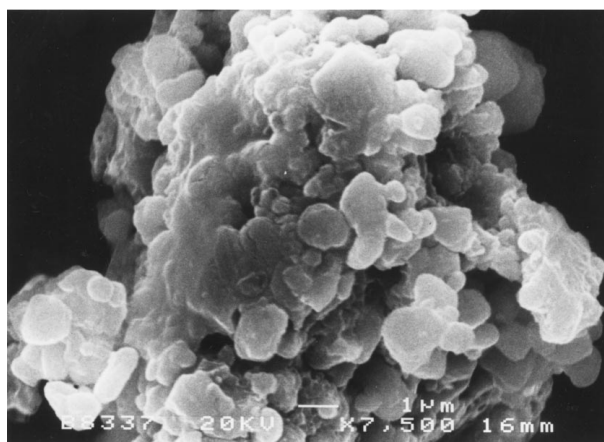
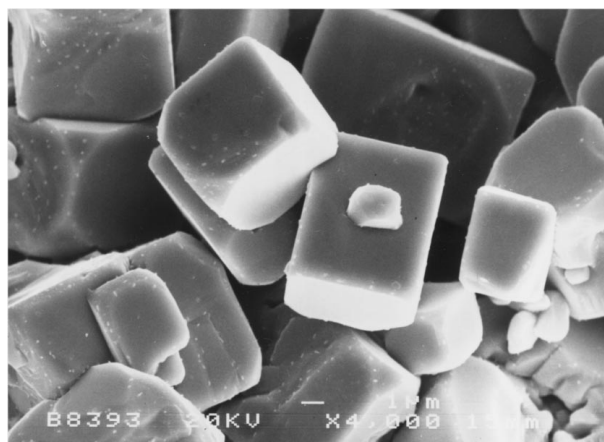


Figure 9 X-ray patterns of the gel calcined at 1000 °C for 8 h (a) and the powder sintered at 1450 °C for 2 h (b); * = SnO₂.



(a)



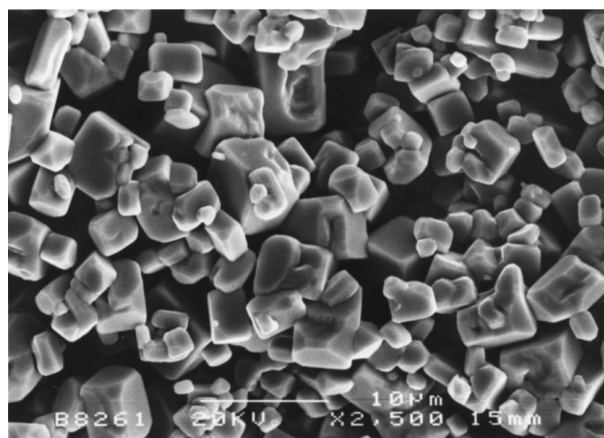
(b)

Figure 10 Microstructure of the ethoxide gel-derived BaSnO₃: (a) morphology of the dried gel (b) soaked for 24 h at 1200 °C.

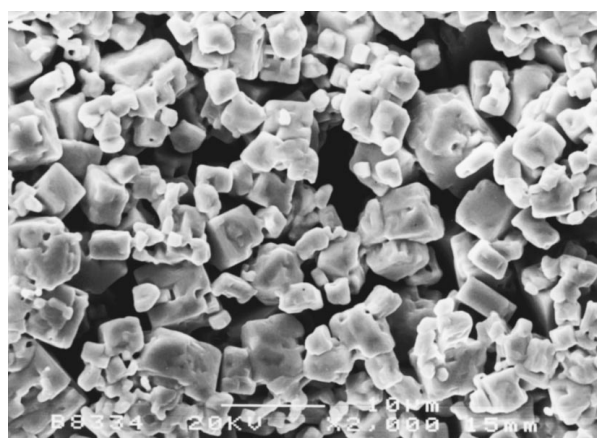
3.3. BaSnO₃ gel

3.3.1. Characterization of dried and calcined gel

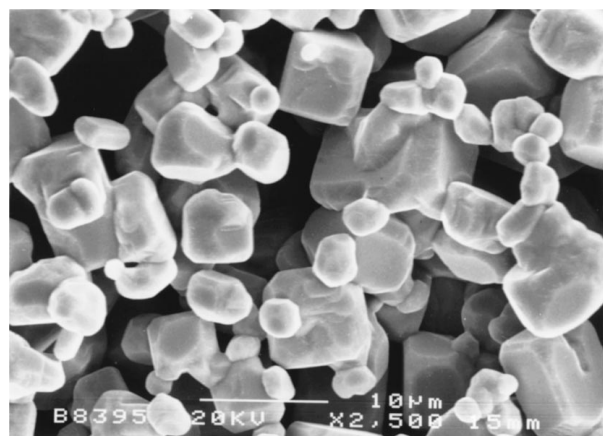
The infrared spectroscopic signatures of the ethoxide-derived gels (dried and those calcined up to 900 °C), revealed that BaSnO₃ began to form in gel subjected to calcination at 800 °C and the transformation was complete at 900 °C. The X-ray diffraction patterns of the dried gel and those calcined at 400, 600 and 800 °C for 2 h showed that a partial crystallinity (but not the compound formation) appeared to set in at about ~400 °C. However, the gradual transformation of the



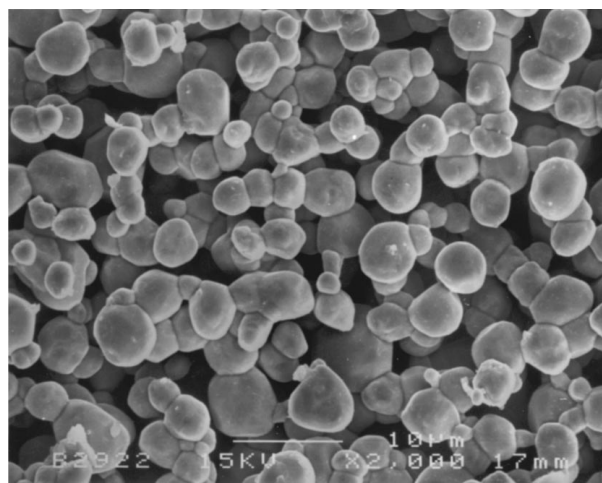
(a)



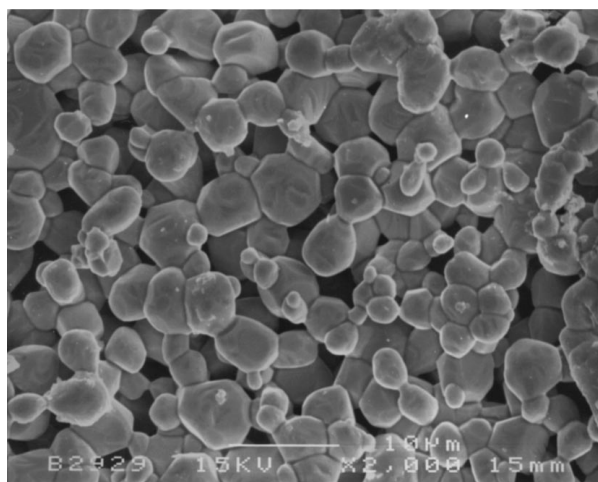
(b)



(c)



(d)



(e)

Figure 11 Microstructure of ethoxide gel-derived BaSnO_3 soaked at (a) $1300\text{ }^\circ\text{C}/6\text{ h}$, (b) $1300\text{ }^\circ\text{C}/12\text{ h}$ (c) $1400\text{ }^\circ\text{C}/6\text{ h}$ (d) $1450\text{ }^\circ\text{C}/2\text{ h}$ and (e) $1500\text{ }^\circ\text{C}/2\text{ h}$.

gel into the target phase of BaSnO_3 did not begin until $600\text{ }^\circ\text{C}$ and above. This corroborates the IR data that BaSnO_3 derived from ethoxide precursor gel could only be obtained in crystalline form after calcination above $800\text{ }^\circ\text{C}$. Interestingly, the minor impurity SnO_2 phase detected in the powders calcined at $1000\text{ }^\circ\text{C}$ for 8 h disappeared totally and ‘phase pure’ BaSnO_3 is obtained in the body at $1450\text{ }^\circ\text{C}$ for 2 h. This is shown in Fig. 9. A value of 4.112 \AA for the unit cell (cubic symmetry) lattice parameter computed from the d-spacings, compares well with 4.11 \AA reported in the literature.

3.3.2. Microstructure in sintered bodies

The morphology of the dried BaSnO_3 gel in shown in Fig. 10a. The microstructure of the pellets sintered at $1200\text{ }^\circ\text{C}$ for 24 h is shown in Fig. 10b. The perfectly cubic geometry of the grains is identical to that observed in the sintered BaSnO_3 bodies derived from solid state reaction (SSR) and self-heat-sustained (SHS) techniques [11]. Fig. 11a and b illustrate the microstructural features in the samples sintered at $1300\text{ }^\circ\text{C}$ for 6 and 12 h, respectively. The microstructure resulting up on sintering at $1400\text{ }^\circ\text{C}$ for 6 h is shown in

Fig. 11c. It is interesting to recall that in the case of SSR derived BaSnO_3 , the porous 'sugar cube' features could not be eliminated in samples sintered up to 1600°C . On the other hand, a typical dense microstructure consisting of spherical grains was obtained when the SHS derived compacts were sintered at 1600°C for 2 h. It can be clearly seen from Fig. 11 a–c that while the grain morphology continues to be 'sugar cube' type, the grain size distribution is rather large. Only at the higher sintering temperature (viz., $1400^\circ\text{C}/6$ h), smoothening of the grain edges sets in and some of the grain acquire the spherical shape, typical of the ceramic microstructure. There still remains, however, a significant amount of porosity in the structure. Nevertheless, the microstructural features change dramatically in samples soaked for 2 h at 1450 and 1500°C (Fig. 11d and e). The grains are mono-sized and near spherical with non-existent 'sugar cube' features. One difference between the microstructures shown in Fig. 11 and those developed in SSR and SHS derived BaSnO_3 is that the sol-gel samples are denser relative to the later sintered under identical conditions. It is therefore likely that a fully dense body could be obtained from sol-gel derived BaSnO_3 at temperatures lower than 1600°C .

4. Conclusions

The sol-gel synthesis route yielded very fine, homogeneous and reactive hydrolyzed precursors, with spherical grain morphology, characteristic of sol-gel derived materials. From these gels, phase pure MSnO_3 could be formed at temperature as low as 600°C in just 2 h (in the case of SrSnO_3). In the case of CaSnO_3 , the temperature of formation of crystallites from the gel was dependent on the nature of the organometallic used as the starting material; the ethoxide gel transformed into crystalline form up on calcining at 600°C for 4 h, while that derived from acetates could result in compound formation upon calcination at $800^\circ\text{C}/4$ h. In the case of barium analogue, compound formation seemed to have begun at temperatures above 600°C .

Infrared spectroscopy and X-ray analyses of various samples with different thermal history helped in identifying the reaction process and the stage where amorphous gel to crystalline phase transition occurred. Microstructural examination of the sintered bodies revealed that more favorable characteristics were obtained in ethoxide derived CaSnO_3 in comparison to the acetate analogue, which possessed better green powder characteristics. In the case of BaSnO_3 , the 'sugar cube' morphology was found to be an inherent property of the system and better densification at temperature lower than 1600°C is anticipated.

Acknowledgments

The authors wish to thank Dr. S. A. Akbar of the Department of Materials Science and Engineering, The Ohio State University, USA, for carrying out XRD on some of the samples. They also thank Dr. M. K. Vidyadharan, Ms. Azilah Abdul Jalil and Mr. Ho Oi Kuan of the Institute of Bioscience (UPM) for generously allowing the usage of their electron microscopy facilities. Encouragement by Dr. A. Q. Khan of KRL, Pakistan, for this collaborative effort is gratefully acknowledged.

References

- (a) J. M. HERBERT, "Ceramic Dielectrics and Capacitors" (Gordon and Breach Science Publishers, Philadelphia 1985); (b) R. BUCHANAN, "Ceramic Materials for Electronics" (Marcel Dekker, New York 1986); (c) A. J. MOULSON and J. M. HERBERT, "Electroceramics: Materials, Processing, Applications" (Chapman and Hall, New York, 1990).
- Y. SHIMIZU, M. SHIMABUKURO, H. ARAI and T. SEIYAMA, *J. Electrochem. Soc.* **136** (1989) 1206.
- U. LUMPE, J. GERBLINGER and H. MEIXNER, *Sensors and Actuators B* **26/27** (1995) 97.
- R. OSTRICK, M. FLEISCHER and H. MEIXNER, *J. Am. Ceram. Soc.* **80** (1997) 2153.
- P. T. MOUSLEY, A. M. STONEHAM and D. E. WILLIAMS, in "Techniques and Mechanisms in Gas Sensing," edited by P. T. Moseley, J. O. W. Norris and D. E. Williams (Adam Hilger, Bristol, 1991) Ch. 4.
- L. M. SHEPPARD, *Adv. Mater. Processes* **2** (1986) 19.
- O. PARKASH, K. D. MANDAL, C. C. CHRISTOPHER, M. S. SASTRY and D. KUMAR, *J. Mater. Sci. Lett.* **13** (1994) 1616.
- K. D. MANDAL, M. S. SASTRY and O. PARKASH, *ibid.* **14** (1995) 1412.
- (a) S. UPADHYAY, O. PARKASH and D. KUMAR, *ibid.* **16** (1997) 1330; (b) S. UPADHYAY, A. K. SAHU, D. KUMAR and O. PARKASH, *J. Appl. Phys.* **84** (1998) 828.
- A.-M. AZAD, in Proceedings of 5th International Symposium on Advanced Materials, September 21–25, 1997, Islamabad, Pakistan, edited by M. A. Khan, A. Haq, K. Hussain and A. Q. Khan (Dr. A. Q. Khan Research Laboratories, Kahuta, Pakistan 1998) p. 110.
- A.-M. AZAD and N. C. HON, *J. Alloys Comp.* **270** (1998) 95.
- A.-M. AZAD, L. L. W. SHYAN and P. T. YEN, *ibid.* **282** (1999) 109.
- A.-M. AZAD, L. L. W. SHYAN and M. A. ALIM, *J. Mater. Sci.* **34** (1999) 1175.
- Idem.*, *ibid.* **34** (1999) 3375.
- A.-M. AZAD, L. L. W. SHYAN, P. T. YEN and N. C. HON, *Ceram. Int.*, in press.
- R. A. NYQUIST and R. D. KAGEL, "Infrared Spectra of Inorganic Compounds" (Academic Press, New York, 1971) p. 108, 128.

Received 13 April 1999
and accepted 11 April 2000